Design and Optimisation of a Footfall Energy Harvesting System

James M Gilbert and Farouk Balouchi
Department of Engineering, University of Hull, Hull, HU6 7RX, UK, Email: j.m.gilbert@hull.ac.uk

Keywords: Energy Harvesting, Energy Scavenging, Footfall, Efficiency, Energy Conversion.

ABSTRACT:

The scavenging of electrical energy from normal human activity has a number of attractions and footfall energy is seen as one of the most attractive sources. However, footfall motion is characterised by relatively large forces and low velocities and this makes it inherently poorly matched to electromagnetic generators which operate most efficiently at high speeds. In order to achieve an efficient velocity amplification, a novel mechanism has been developed which makes use of a spring and flywheel as energy storage elements and a 'striker' mechanism which controls energy storage and release. This energy harvesting mechanism is capable of being used either in footwear or under a floor. In this paper the structure of the proposed mechanism is described, the optimisation of the system parameters, based on a dynamic model, is discussed and experimental results for an under-floor system are presented.

This research received no specific grant from any funding agency in the public, commercial, or not-for-profit sectors.

INTRODUCTION

There are a number of applications in which it is desirable to provide modest amounts of electrical energy in locations where it is not cost effective to connect to existing electrical power infrastructure and where stored energy sources, such a batteries, are not convenient (Priya and Inman, 2009). In these circumstances the generation of power from ambient energy sources or fields is an attractive solution. Such energy sources include light, thermal gradients and vibration (Priya and Inman, 2009), (Gilbert and Balouchi, 2008). A further source of energy which has been given some consideration is human movement. Starner (1996) analysed the various sources of power associated with human activity and demonstrated that lower limb movement provided the largest source of energy. While leg movement has the potential to generate of the order of 300W, extracting this level of power would be a significant impediment to normal activity. Devices which aim to extract a lower level of power from knee flexure without significantly affecting the user are described in (Donelan et al., 2008). Several authors have considered utilising footfall as a source of energy since it may be argued that energy is normally dissipated in the footwear and flooring due to their compressibility. Starner (1996) estimated that approximately 67W is available from footfall although this does not consider the comfort of the user. A number of conversion techniques have been investigated including

piezoelectric materials (Shenck and Paradiso, 2001), Electroactive polymers (EAP) (Pelrine, 2001, 2002) and electromagnetic conversion (Kymissis, 1998). It has generally been found that piezo materials give relatively poor levels of output power, EAPs are reported to give a good level of power but have uncertain reliability and electromagnetic conversion is reported to give moderate power levels and greater reliability. A comparison of energy harvesting technologies is presented in (Gilbert. and Balouchi, 2008).

A more limited number of researchers have also considered embedding energy harvesting devices within surfaces to capture energy from pedestrian and vehicular traffic. The majority of floor mounted footfall energy harvesters are based around piezo conversion. The level of power generated in these devices is not clearly specified but is believed to be relatively modest. For example the device reported in (Takefuji, 2008a,b) generates 0.14mJ per step from a single generator. Other under floor generator systems are described in the popular media, they are not described in the scientific literature and so the performance cannot be verified. Energy harvesting from vehicular traffic using electromagnetic conversion, with a form of flywheel mechanism, for has also been considered (Highway Energy Systems Ltd) but once again, reliable figures for output power are not available.

The novel mechanism described in this paper aims to improve the efficiency of velocity amplification by storing input energy in a spring before transferring it to a flywheel and then to a generator. This process which is controlled by a ‘striker;’ or trigger mechanism, effectively decouples the input and output sides of the device, allowing a relatively efficient energy conversion,

The paper is organised as follows: firstly the design constraints on an under floor (or under stair) device are discussed and the proposed new mechanism introduced. A mathematical model of the behaviour of the mechanism is developed as a basis for identifying system parameters which give optimum performance. This is followed by experimental results and discussion and conclusions.

CONVERSION MECHANISM DESIGN

In this section we describe, in more detail, the constraints upon the design of an under floor energy harvesting device and outline the proposed system structure and operation.

Design Considerations

It is desirable that an under floor energy harvesting device should have minimal impact on the user. Thus the possible displacement of the floor must be restricted to an acceptable amount. The amount considered acceptable may depend on the context (for instance, when walking on a carpeted floor a significant deflection of the floor surface is expected while when walking on a solid stone floor one would not expect any significant deflection). From initial experimental studies it is believed that a deflection of the order of 10mm is acceptable in most situations. Taken over the entire period of the gait cycle, this movement represents a low average velocity (albeit at a relatively high force). Thus there is an inherent mismatch when attempting to use electromechanical conversion to

harvest energy from human activity since the majority of electromagnetic generators operate most efficiently at relatively high speeds. The conventional method of adjusting speed and torque is to use gears but these incur power losses and these losses generally increase as the input/output speed ratio increases. In addition, the peak impact forces involved in footfall can be large, especially during running, and so large gears, capable of transmitting these peak forces, are required. Larger gears generally imply larger friction losses, thus reducing efficiency further.

The proposed mechanism aims to achieve speed conversion in a more energy efficient manner by making use of the pulsed nature of the input energy and using energy storage elements to allow more gradual conversion of mechanical to electrical energy.

Proposed design

The proposed design is shown in Figure 1, along with the key phases of its operation. It is composed of a 'striker' mechanism which is coupled to the floor and so undergoes a vertical displacement when a pedestrian steps on the floor. The striker presses against the pivot arm causing it to rotate and twist the torsional spring which is attached to it. Once the striker approaches the end of its travel the pivot arm is released so that the spring may return to its starting position. The spring is coupled, via a sprag (one way) clutch, to a flywheel and generator in such a way that when being wound up there is no torque transfer but when the spring unwinds, it drives the flywheel and generator. In addition, the sprag clutch allows the flywheel to continue to rotate once the spring stops unwinding. When the weight of the pedestrian is removed from the floor, the striker is able to move up again and the ratchet mechanism passes the end of the pivot arm and returns to its initial position, ready for the next cycle. Thus the spring and flywheel are able to convert the short pulse of input energy into an extended pulse of energy applied to the generator. This prolonging of the pulse, and the associated reduction in peak power, allows smaller mechanical elements and a smaller generator to be used, typically with lower energy losses.

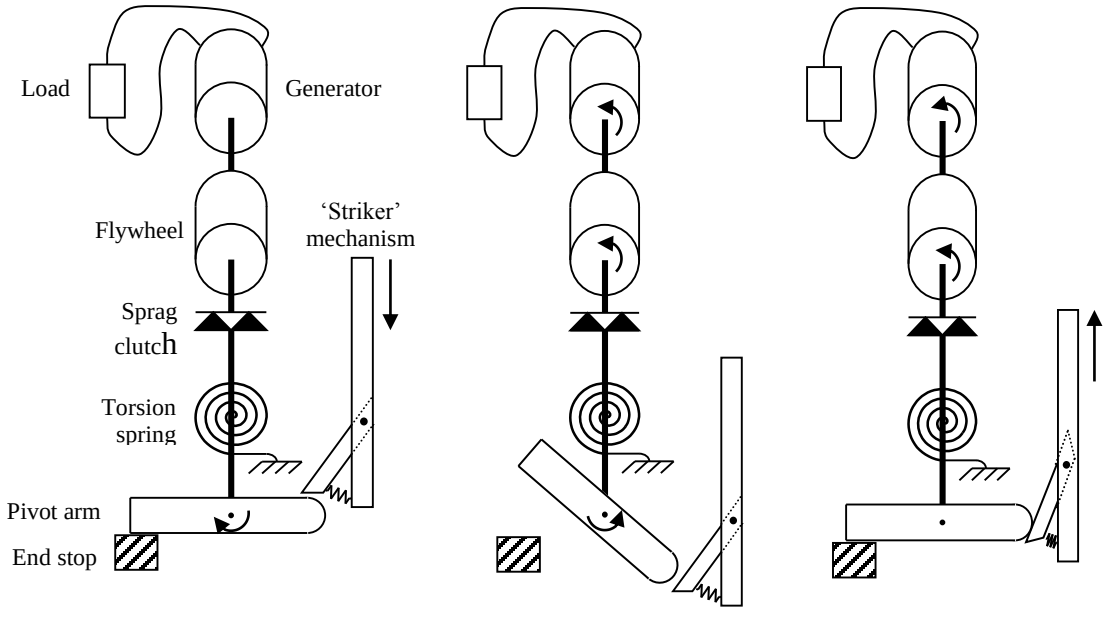

Phase 1 Phase 3 Phase 4

Figure 1 Structure and operating sequence of proposed converter mechanism

This principle of pulsed energy conversion is similar to that used in electrical switched mode converters (Gilbert et al, 1996), (Hassan, Gilbert and Ishak, 2008) and is referred to as a ‘flyback’ converter by analogy to these electrical converters. In electrical converters the input energy is stored in an inductor (spring) under the control of a switch and is then transferred through a diode (clutch) to a capacitor (flywheel) at a higher voltage (speed) than the input. In the electrical domain, conversion efficiency of the order of 90% can be achieved.

The behaviour of the system during a single footfall cycle may be split into four phases (see Figure 1) as described below. The evolution of the key variables in each phase is illustrated in Figure 2.

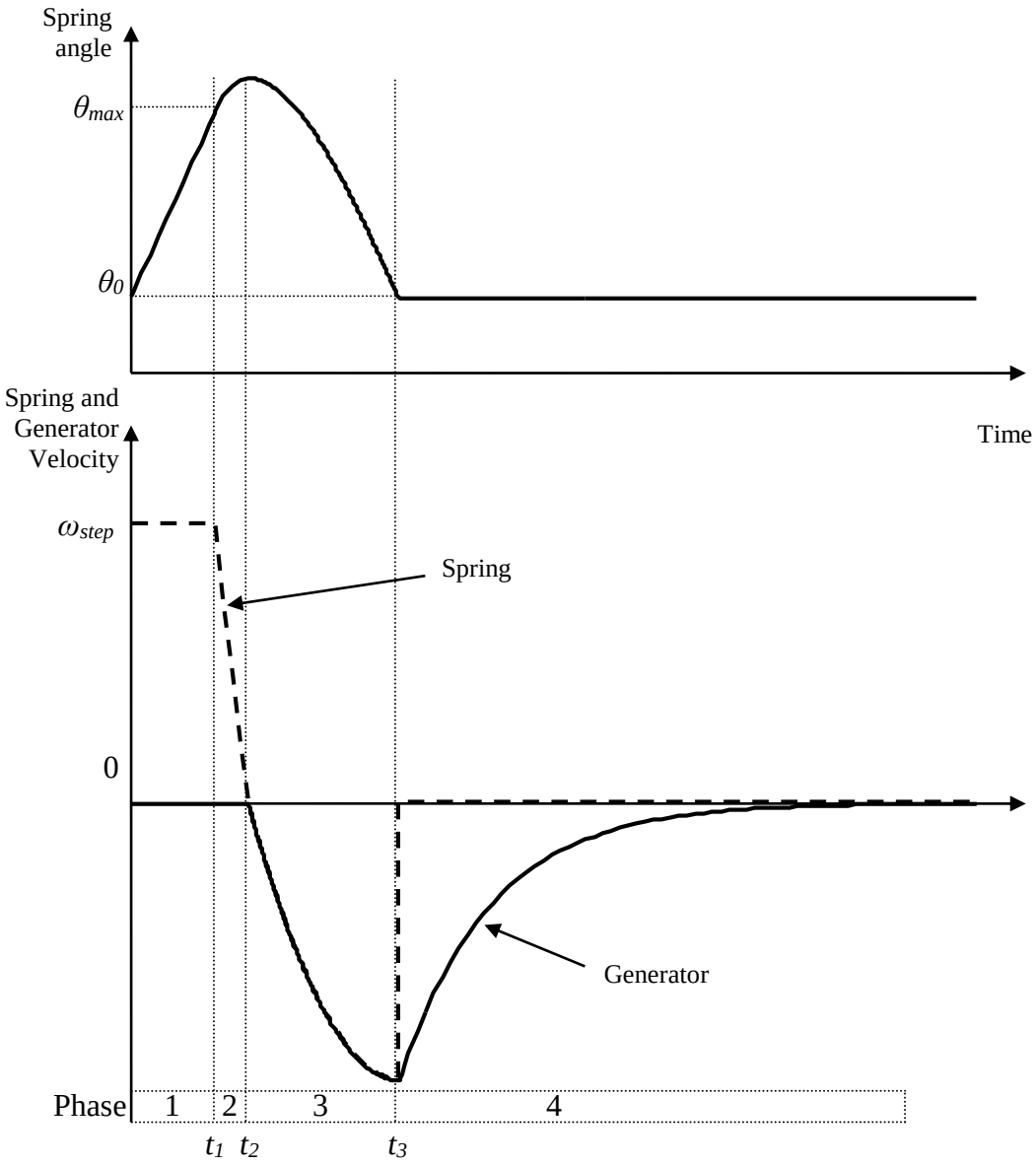

Figure 2 Evolution of variables during energy conversion cycle showing 4 phases of operation

Operation Phases:

1. **Spring windup during footfall.** As the pedestrian deflects the floor, the striker causes the pivot arm to rotate from an initial angle, θ_0 to a maximum angle θ_{max}. It is assumed for illustration purposes that the spring winds at a constant rate ω_{step}. In the subsequent analysis, it will be assumed that the angles θ_0 and θ_{max} are small and are symmetrically arrange around the horizontal position so that the effective radius is constant and the torque applied to the spring is proportional to the force applied to the striker. Once the angle θ_{max} is reached, the striker clears the end of the pivot arm and the spring is released, beginning phase 2.
2. **Spring velocity drops to zero.** At the beginning of phase 2 the spring is rotating with velocity ω_{step} but once released from the striker mechanism, the spring is decelerates due to the torque generated in the spring. During this phase the sprag clutch does not transfer any torque. Once the spring velocity passes through zero the sprag clutch engages and phase 3 begins.
3. **Spring drives generator.** Once the sprag clutch engages, the spring drives the flywheel and generator, causing them to accelerate. During this phase, the spring is accelerating both its own inertia and that of the flywheel/generator and so the acceleration is lower than in Phase 2. The spring will drive the flywheel/ generator until the spring end stop is reached (at the angle θ_0). This causes the mechanism to move to Phase 4.
4. **Rundown of flywheel.** Once the spring reaches the end stop, the spring velocity drops rapidly to zero but the flywheel continues to spin, driving the generator. The flywheel decelerates under the influence of friction and the reflected torque from the generator.

At some stage, the foot will be lifted from the floor, the striker mechanism slips past the end of the pivot arm and the input mechanism resets. This is not shown in Figure 2.

This mechanism has several advantages over more conventional gearing mechanisms. During footfall the applied force is only used accelerate the striker mechanism and to twist the spring. These parts may be designed to have low mass/inertia and hence the dynamic forces during impact are not significant compared to the spring forces. The sprag clutch decouples the input and output side of the mechanism so that they may largely be designed separately, allowing greater freedom in the choice of parameters.

PERFORMANCE MODEL

In order achieve good efficiency from this mechanism, it is necessary to select the system parameters carefully and for this purpose it is helpful to develop a model of its behaviour. The model for each phase of operation will be describer in turn. A number of assumptions will be made in the development of the model. It will be assumed that the spring operates in a linear manner (obeys Hooke's law). It will be assumed that the friction affecting the spring, flywheel and generator may be modelled as being composed of a viscous element and a coulombic element. Stiction will be neglected since the mechanism may be designed so that the actuating torques are sufficient to overcome

stiction torques. The friction of the free wheeling sprag clutch will be combined with the coulombic and viscous elements of the spring and flywheel.

Phase 1 - Spring windup during footfall ($0 < t < t_1$). The precise velocity and displacement profile (and associated applied force) during this phase is unimportant in terms of the subsequent behaviour. For simplicity, Figure 2 illustrates the situation where footfall occurs at a constant velocity ω_{step}. What is important is the spring velocity at the point where the input mechanism releases the spring. For the subsequent phases of the behaviour, it will be taken that this velocity is ω_{step}. As will be seen subsequently, it is advantageous to have the spring already under torsion at the beginning of phase 1. If the spring is at an initial angle θ_0 from its equilibrium position then it has a potential energy of:

$$E_0 = \frac{1}{2} k_s \theta_0^2$$

where k_s is the spring constant

At the end of phase 1 the total energy is made up of the spring's potential energy and the spring inertia's kinetic energy. Thus:

$$E_1 = \frac{1}{2} k_s \theta_{\max}^2 + \frac{1}{2} J_s \omega_{step}^2$$

where θ_{max} is the rotation of the spring at the point where it is released
J_s is the moment of inertia of the spring and associated parts

The energy extracted from the pedestrian is:

$$E_{in} = \frac{1}{2} k_s \left(\theta_{\max}^2 - \theta_0^2\right) + \frac{1}{2} J_s \omega_{step}^2 \quad (1)$$

Phase 2 - Spring velocity drops to zero ($t_1 < t < t_2$). During this phase the spring behaviour is governed by the equation:

$$J_s \ddot{\theta}_s = -k_s \theta_s - B_s \dot{\theta}_s - D_s \operatorname{sgn}\left(\dot{\theta}_s\right) \quad (2)$$

where θ_s is the angle of rotation of the spring
B_s is the viscous friction coefficient associated with the spring
D_s is the coulomb friction coefficient associated with the spring

with initial conditions $\theta_s(t_1) = \theta_{\max}$ and $\dot{\theta}_s(t_1) = \omega_{step}$. Phase 2 ends at time t_2 when the spring velocity reaches zero: $\dot{\theta}_s(t_2) = 0$. The spring angle at the end of Phase 2,

$\theta_{s2} = \theta_s(t_2)$ can be determined by solving Equation (2). The energy stored in the system at this time is.

$$E_2 = \frac{1}{2} k_s \theta_{s2}^2$$

Phase 3 - Spring drives generator ($t_2 < t < t_3$). Once the velocity of the spring passes through zero, the sprag clutch connects the spring and flywheel/generator and so the generator velocity, $\dot{\theta}_g$ is equal to the spring velocity $\dot{\theta}_s$. Note that the rotation angles are not necessarily equal since the sprag clutch allows the flywheel/generator to rotate to any position $\theta_g \leq \theta_s$. However, the relative angles remain constant during this phase. The dynamics during Phase 3 are governed by:

$$(J_s + J_g)\ddot{\theta}_s = -k_s\theta_s - (B_s + B_g)\dot{\theta}_s - (D_s + D_g)\text{sgn}(\dot{\theta}_s) - k_t i \qquad (3)$$

where J_g is the moment of inertia of the generator, flywheel and associated parts
B_g is the viscous friction coefficient associated with the generator/flywheel
D_g is the coulomb friction coefficient associated with the generator/flywheel
k_t is the torque constant of the generator
i is the current flowing through the generator and into the load

The generator may be described as a voltage source proportional to angular velocity of the generator and a series resistance (the effect of generator inductance will be neglected in the model). The load will be assumed to be a constant resistance. Thus the generator current is:

$$i = \frac{k_e \dot{\theta}_s}{R_g + R_l} = \frac{k_e \dot{\theta}_g}{R_g + R_l}$$

where k_e is the emf constant of the generator (equal to k_t)
R_g is the winding resistance of the generator
R_l is the load resistance

The initial conditions at the beginning of phase 3 are $\dot{\theta}_s(t_2) = 0$ and $\theta_s(t_2) = \theta_{s2}$. Phase 3 ends when the spring angle returns to the value at the start of phase 1, $\theta_s(t_3) = \theta_0$. At this point the spring and generator velocities are equal $\dot{\theta}_s(t_3) = \dot{\theta}_g(t_3) = \dot{\theta}_{g3}$ and can be determined from the solution of Equation (3).

Phase 4 - Rundown of flywheel ($t_3 < t < t_4$). When the spring reaches its end stop it is assumed that it stops instantaneously and the flywheel continues to rotate. The precise behaviour of the spring during this phase is unimportant since it does not affect the output power. The dynamics of the flywheel and generator during phase 4 are described by:

$$J_g\ddot{\theta}_g = -B_g\dot{\theta}_g - D_g \operatorname{sgn}\left(\dot{\theta}_g\right) - \frac{k_t k_e \dot{\theta}_g}{R_g + R_l} \tag{4}$$

The initial conditions for phase 4 are $\theta_g(t_3) = \theta_0$ and $\dot{\theta}_g(t_3) = \dot{\theta}_{g3}$.

Power is generated and transferred to the load resistance during phases 3 and 4 and so the total energy delivered to the load is:

$$E_{out} = R_l \int_{t_2}^{t_4} i(t)^2 dt \tag{5}$$

Based on this model it is possible to model the energy delivered to the load for given input characteristics and hence maximise the output energy. The result of this optimisation will be discussed in the following section.

PARAMETER OPTIMISATION

In order to optimise the power output from the system the most appropriate system parameters must be determined given the constraints on the system. It is important to note that the aim is to optimise the output electrical energy rather than to optimise the conversion efficiency. To maximise the output energy we wish to extract as much energy from the pedestrian as possible and then convert this to output energy as efficiently as possible. Thus we will first consider the energy extracted from the pedestrian.

As shown in Equation (1), the energy derived from the pedestrian depends on the force applied by the foot, the associated displacement of the spring and the angular velocity of the spring rotation. As will be seen later, it is desirable to minimise the moment of inertia of the spring and so the final term in equation (1) will be ignored. The force applied during walking clearly depends on the mass of the pedestrian but also on their gait. During normal walking the peak reaction forces are approximately 25% greater than body weight while during running the peak reaction forces are typically 2.75 to 3 times body weight (Trew and Everett, 2001). In a general environment there will be a range of pedestrians each having a different body weight and gait. For the purposes of this paper however, we will assume a fixed body weight, Mg (where M is the pedestrian mass and g is the gravitational constant) and will assume that the reaction force is equal to that body weight. The deflection in the floor surface also determines the input energy but in order to avoid discomfort or distraction for the pedestrians this deflection must be limited. As noted previously, the acceptable limit appears to be approximately 10mm in most environments. The relationship between the angular displacement of the spring and the torque is shown in Figure 3. The additional potential energy stored in the spring as a result of increasing the angle from θ_0 to θ_{max} is equal to the shaded area in Figure 3 which is given by:

$$E_p = \frac{1}{2} k_s \left(\theta_{\max}^2 - \theta_0^2 \right) \tag{6}$$

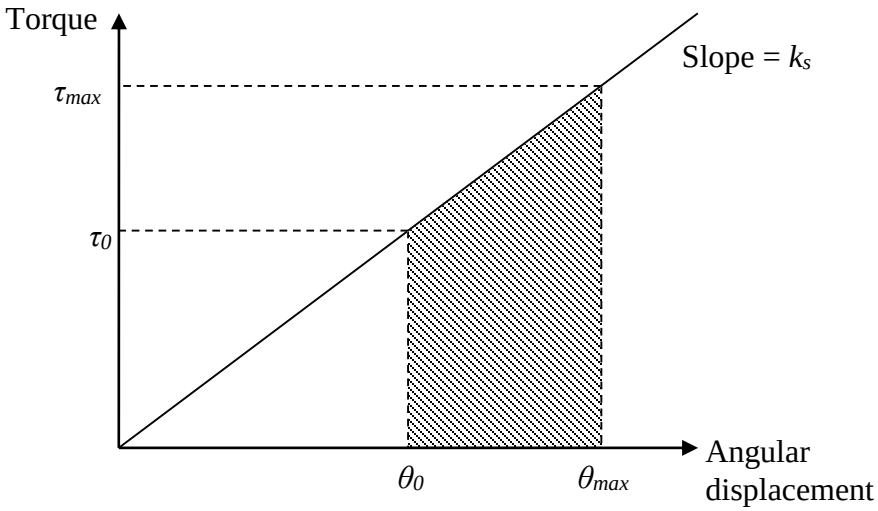

Figure 3 Torque-angle relationship for spring

We wish to maximise this energy while satisfying the constraints:

$$k_s \theta_{\max} \le Mgr$$

and

$$\theta_{\max} - \theta_0 \le \frac{d_{\max}}{r}$$

where r is the length of the pivot arm and d_{max} is the maximum allowable deflection of the floor. The maximum energy occurs if $k_s \theta_{\max} = Mgr$ and $\theta_{\max} - \theta_0 = \frac{d_{\max}}{r}$ in which case Equation (1) (ignoring the final term) may be written as:

$$E_{in} = k_s \left(\theta_{\max} - \theta_0 \right) \left[\theta_{\max} - \frac{1}{2} \left(\theta_{\max} - \theta_0 \right) \right] = Mgd_{\max} - \frac{1}{2} k_s \left(\frac{d_{\max}}{r} \right)^2 \tag{7}$$

This reaches a maximum value of $E_{in} = Mgd_{\max}$ as $k_s \to 0$. In this case $\theta_{\max} \to \infty$ so that the relationship $k_s \theta_{\max} = Mgr$ is maintained. In other words, the shaded area in Figure 3 approaches a rectangular shape. Thus the desirable spring characteristics are that it should have low stiffness but should have a large pre-load, θ_0. It should however be noted that as $k_s \to 0$ and $\theta_{\max} \to \infty$ the total amount of energy stored in the spring increases and hence the amount of material required to make the spring increases. This, in turn, implies an increase in the mass and moment of inertia of the spring. The increase in

inertia is undesirable (as will be seen later) and so a trade-off must be reached between spring inertia and input energy capture.

The inertia of the spring is important because, at the end of phase 3, the spring and the generator are rotating with the same angular velocity, ω_g and the energy is:

$$E_3 = \frac{1}{2}\left(J_s + J_g\right)\omega_g^2$$

while immediately afterwards, at the beginning of phase 4, the velocity of the generator is ω_g but the velocity of the spring is zero and so the energy is:

$$E_3^+ = \frac{1}{2} J_g \omega_g^2$$

Thus, a proportion of the energy $\frac{J_s}{J_s + J_g}$ is lost. To minimize this loss, J_s must be minimized.

The losses due to friction and due to the internal resistance of the motor are more complex and are related to one another. Clearly, if friction could be eliminated, then the associated losses would also be zero but reducing friction typically requires more precise and hence more expensive construction or special devices, such as air or magnetic bearings, which themselves consume power. The spring friction terms B_s and D_s only affect behaviour during phase 2 and 3 but not phase 4. Because of this, the relationship between B_s, D_s and efficiency is not significantly affected by the load resistance. The energy losses during phase 2 and 3 associated with these terms increase monotonically with B_s, and D_s. Thus, maximising the output energy can be achieved by minimising these friction coefficients. Similarly, increasing the spring inertia, J_s casues increased energy losses during phase 2 and 3.

The effect of the generator friction terms is rather more complex. The transfer of energy from the generator to the load, which occurs during phase 3 and 4, depends on the internal resistance of the generator and the load resistance. A general relationship between load resistance and efficiency $\left(E_{out}/E_{in}\right)$ cannot be determined analytically but may be determined numerically, as shown in Figure 4 for a number of friction coefficient values.

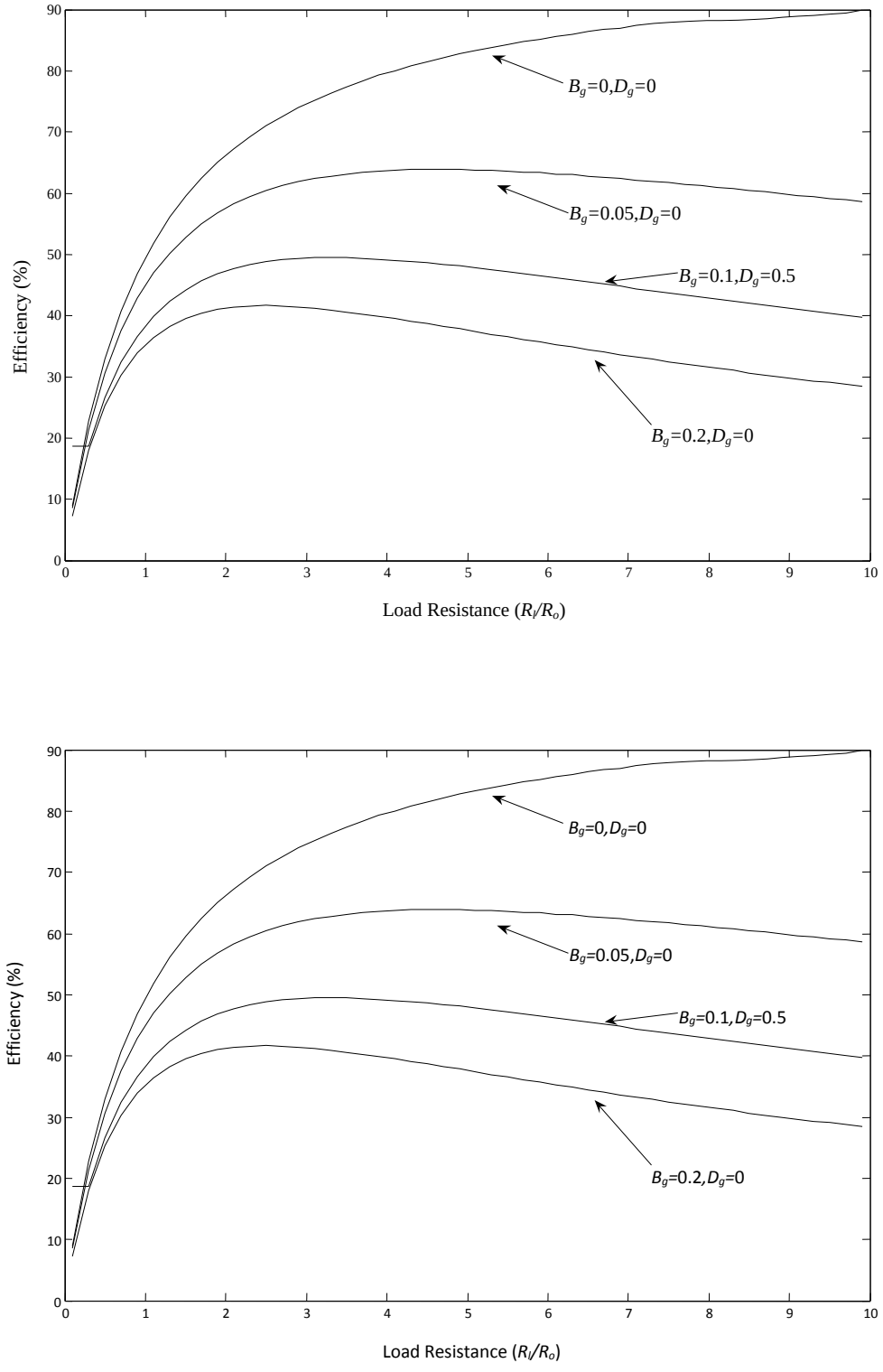

Figure 4 Effect of load resistance on efficiency for different friction coefficients

It can be seen that, as expected, as the friction increases, the system efficiency decreases but it can also be seen that the load resistance for which the efficiency is maximized

depends on the friction coefficients. In all cases, the load resistance for maximum efficiency is significantly higher than the generator internal resistance.

EXPERIMENTAL RESULTS

In order to assess the practical viability of the proposed mechanism, a prototype device has been constructed as shown in Figure 5. In this case the mechanism is actuated through a stair tread rather than being mounted beneath a floor, allowing it to be more easily viewed and instrumented. This prototype is 450mm long and the striker mechanism has a height of 120mm but it has not been designed to be compact. The potential for miniaturisation is outlined in the discussion section. The generator used is a precision DC motor (Portescap) and incremental optical encoders, connected to a PC, are used to monitor spring and flywheel position and velocity. Input energy is measured using a load cell and displacement transducer on the striker mechanism.

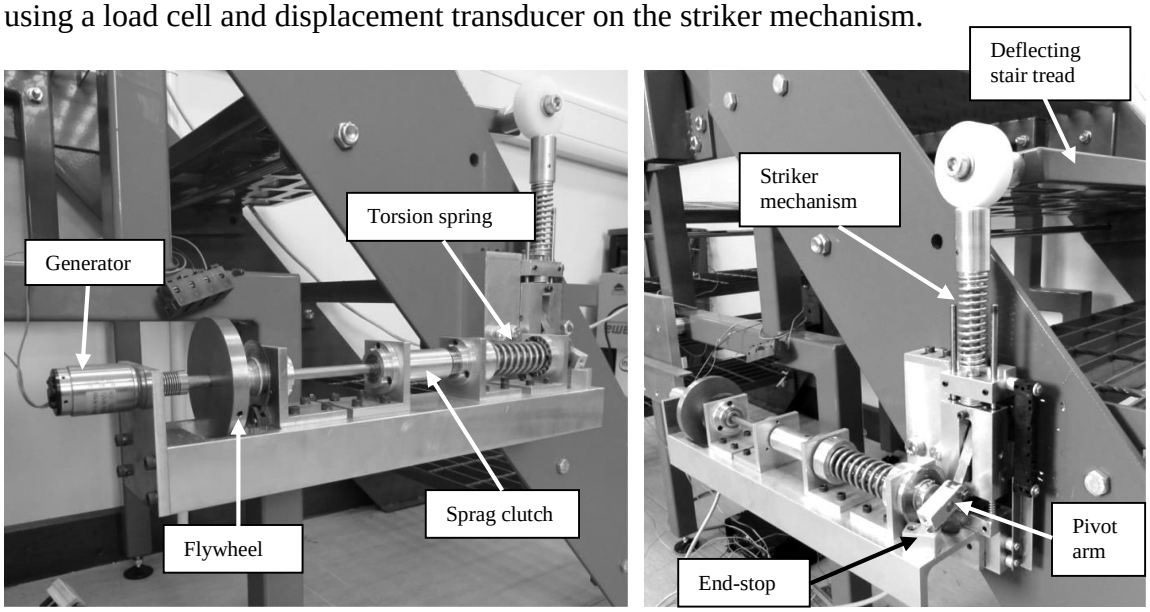

Figure 5 Prototype mechanism mounted on a stair tread

Model Validation

The parameters of the prototype mechanism have been derived from a combination of data sheet information, physical measurement for parameters such as moment of inertia and spring constant and by fitting the simulation to measurements of dynamic behaviour of the system for the friction parameters. The parameters are listed in Table 1.

Parameter	Symbol	Value	Units
Spring constant	k_s	1.62	$N{\cdot}m{\cdot}rad^{-1}$
Moment of inertia of spring mechanism	J_s	$25x10^{-6}$	$kg{\cdot}m^2$
Viscous friction coefficient of spring mechanism	B_s	$5x10^{-6}$	$N{\cdot}m{\cdot}s{\cdot}rad^{-1}$
Coulomb friction constant of spring mechanism	D_s	$1x10^{-6}$	$N{\cdot}m$

Moment of Inertia of flywheel/generator*	J_g	1.6×10^{-4}	$kg \cdot m^2$
Viscous friction coefficient of flywheel/generator	B_g	5×10^{-6}	$N \cdot m \cdot s \cdot rad^{-1}$
Coulomb friction constant of flywheel/generator	D_g	4.2×10^{-3}	$N \cdot m$
Generator winding resistance	R_g	5.95	Ω
Load resistance*	R_L	14	Ω
Spring pre-load	θ_0	1.27	rad
Spring maximum twist	θ_{max}	2.10	rad

Table 1 Parameters of prototype mechanism. Items marked * are the values used in the model validation but may be adjusted to maximise energy output

There is a good level of agreement between the simulation and the experimental measurements using this set of model parameters, as illustrated in Figure 6 which shows a) the spring position during phases 1, 2 and 3 and b) the generator velocity during phase 4. The duration of the first three phases is much shorter than phase 4 and so cannot readily be shown on the same axes.

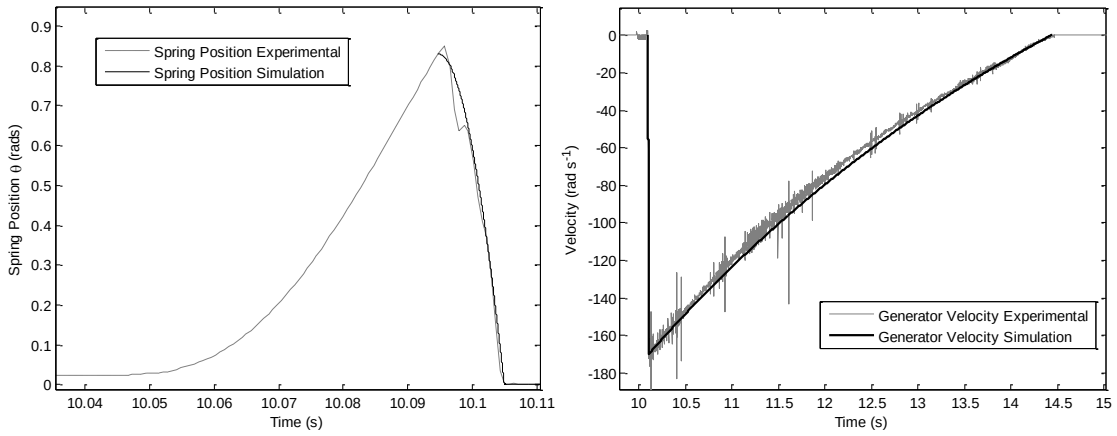

Figure 6 Comparison of experimental and simulated behaviour a) spring position during phase 1,2 and 3 and b) generator velocity during phase 4. Note the difference in timescales for the two plots

The Model continues to give reasonable predictions of performance for a range of parameters. For instance, Figure 7 shows the variation in output energy with load resistance for simulation and experimental measurements. It can be seen that acceptable agreement is achieved. The experimental results indicate slightly lower levels of output energy than the simulation. It is believed that this is due to flexing of the striker mechanism supports which means that the input displacement and hence input energy is lower than that assumed in the simulation.

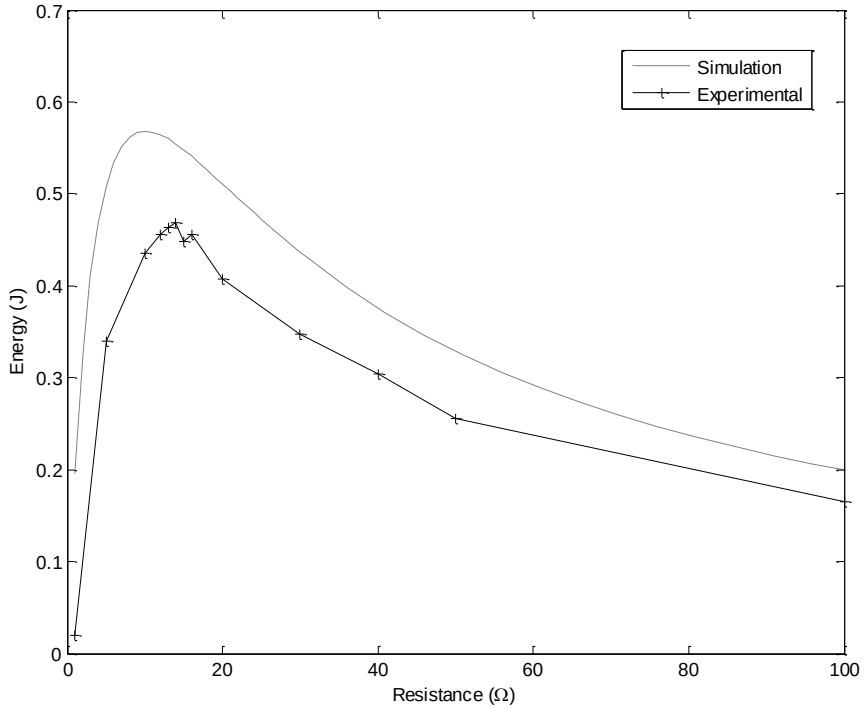

Figure 7 Output energy as a function of load resistance

Effect of Parameter Variation

Based on repeated simulation over a search grid it is possible to estimate the parameters which maximise the energy output for the prototype system. These may be confirmed through experimental studies. As noted previously, it is not possible to arbitrarily alter the frictional characteristics of the mechanism and the minimum spring inertia is limited by its energy storage capability and the strength of the supporting elements. Thus only adjustment of the flywheel inertia and the load resistance are considered here. The optimum values of these parameters were identified as $J_g = 1.6 \times 10^{-4} kg \cdot m^2$ and $R_L = 30\Omega$. These optimum parameters can be confirmed experimentally from Figure 8 which shows in a) the effect of varying flywheel inertia on the delivery of energy to the load. It can be seen that for low inertia ($1.0 \times 10^{-4} kgm^2$) the energy is delivered quickly but the total supplied is lower than for the optimal inertia ($1.6 \times 10^{-4} kgm^2$) while for higher than optimal inertia ($3.4 \times 10^{-4} kgm^2$) the energy is delivered more slowly but again reaches a lower total value. Figure 8 b) shows the energy output as a function of load resistance and it can be seen that the optimum resistance depends on flywheel inertia but that a flywheel inertia of $1.6 \times 10^{-4} kgm^2$ results in the maximum output energy. The peak experimentally measured output energy is 0.46J for a measured input energy of 4J, representing an overall efficiency of 11.5%.

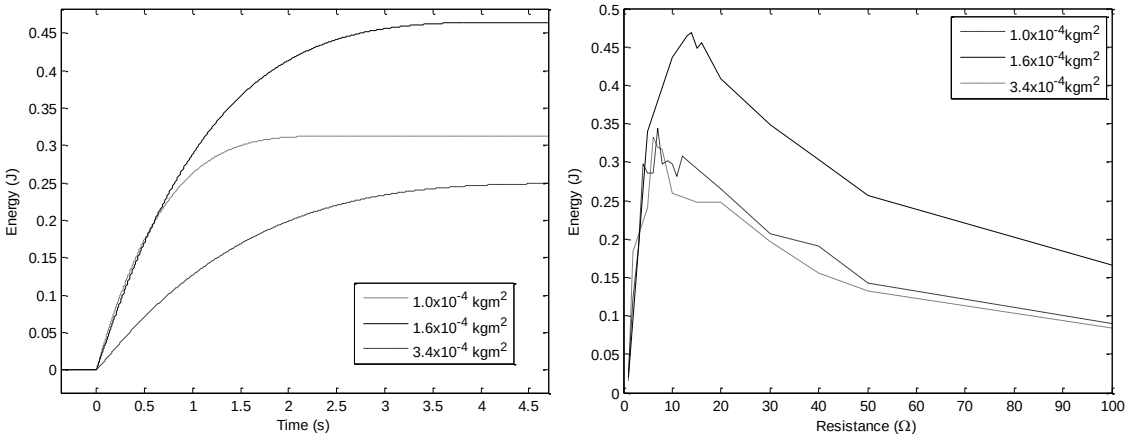

Figure 8 Output energy as a function of load resistance and flywheel inertia a) energy output over time for different flywheel inertia b) output energy as a function of load resistance

Based on the experimental and simulation data, it is possible to determine the causes of the energy losses in the system. This is summarised in Figure 9 which shows the energy losses for optimal system parameters. It may be noted that losses in the striker mechanism account for the largest proportion of the losses while friction in the remainder of the mechanism accounts for the next largest component. Losses resulting from the spring inertia and the winding resistance of the generator are relatively small. Thus, the obvious focus for further work is to reduce losses in the striker mechanism and reduce friction in the remainder of the mechanism.

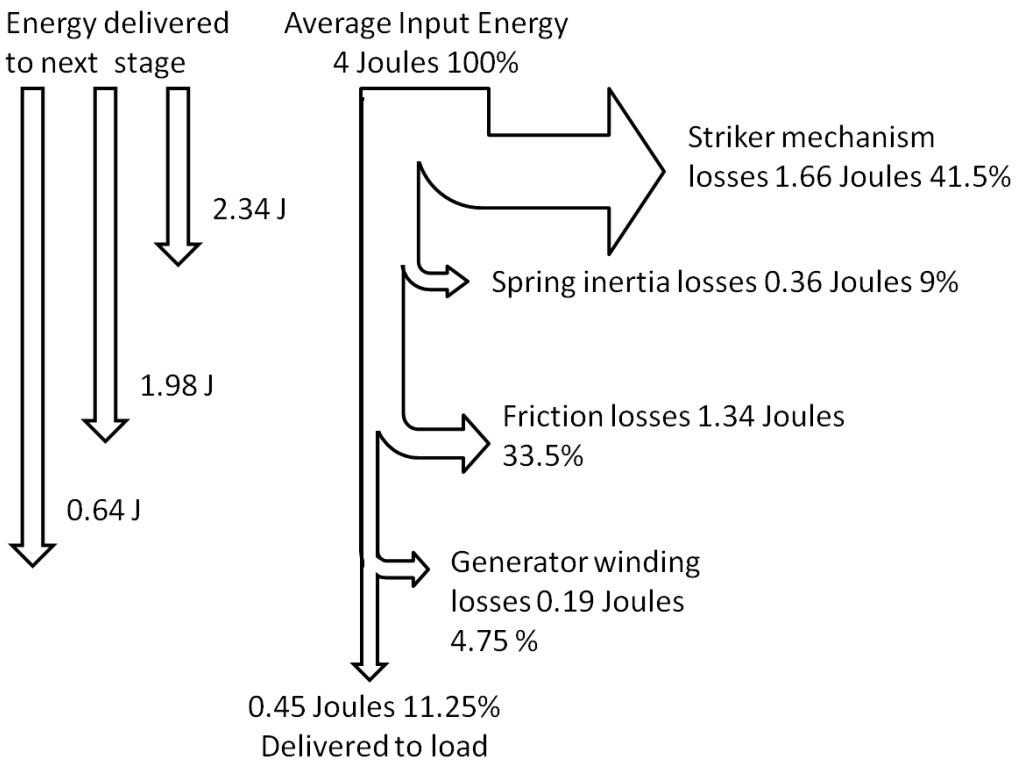

Figure 9 Energy losses within mechanism – absolute value and percentage of input energy

While this mechanism is relatively inefficient, the absolute value of the output energy (0.45J) is higher than that achieved with the majority of footfall harvesting systems. In addition, the peak voltage generated is around 2.5V which is readily converted to an appropriate level for electronic devices.

DISCUSSION

The proposed mechanism provides a means of converting footfall energy to electrical energy in a manner which produces a higher level of energy than the majority of other methods described in the literature.

The detailed simulation model presented allows the major causes of energy loss in the mechanism to be identified and so effort may be directed towards these. It is anticipated that the losses in both the striker mechanism and friction in the flywheel/generator could be significantly reduced by improving the design and through more precise construction. Thus it may be hoped that the efficiency and the output energy may be increased. The model may also be used as the basis for parameter optimisation. In summary, the design aims to fulfil the following objectives:

- Maximise the energy extracted from the pedestrians' footfall through appropriate choice of spring constant and 'pre-load'
- Minimise the inertia of the spring relative to that of the flywheel and generator.
- Minimise friction in the mechanism

- Match the flywheel inertia and load resistance to the other parameters of the system to allow maximum energy extraction

The mechanism has been designed to accept a specified input displacement (in this case 10mm) and applied force (600N). Users of the staircase have reported that although conscious of the movement of the stair tread, they do not find this disturbing, provided they are made aware beforehand that it will move. Studies of the effect on the user of different stair tread movements are planned in order to assess the maximum acceptable movement. Assuming the ground reaction force is equal to the user weight, the input force corresponds to a pedestrian mass of approximately 60kg. For users with lower weight they will not produce sufficient displacement for the striker mechanism to release the spring and so no energy will be transferred to the output. Conversely, for heavier users, they only produce the same displacement, and hence input energy, as a 60kg user. It would be possible to extract more energy from these heavier pedestrians by using a stiffer spring but this would prevent lighter users producing any energy. The choice of optimum 'cut-off' weight depends on the mass distribution among the user population. Selecting this cut-off for particular locations, along with methods of extracting maximum energy from a range of users, is a subject for further study.

An accurate comparison between the power density of the proposed device and other devices described in the literature is difficult due to a lack of detailed information. Based on the information which is presented in the literature, the characteristics of electromagnetic, electro-active polymer and piezo-based footfall harvesters have been estimated and are presented in **Error! Reference source not found.**. These are compared with the characteristics of the flyback converter described in this paper.

Operating principle	Input deflection (mm)	Average output power at 1 step/s (W)	Volume (m^3)	Power density (W/m^3)
PVDF Stave (Shenck and Paradiso, 2001)	-	0.0013	20×10^{-6}	650
PZT Stave (Shenck and Paradiso, 2001)	7	0.0084	34×10^{-6}	250
Geared EM generator (Kymissis, 1998)	30	0.25	160×10^{-6}	1500
EAP Shoe insert (Pelrine, 2001)	-	1	50×10^{-6}	20000
Flyback converter	10	0.45	400×10^{-6}	1100

Table 2 Estimated footfall harvester characteristics

This indicates that the electromagnetic converters offer greater power density than piezo based devices but that they typically require a input greater deflection. The power density for the EAP appears to be the highest of those considered but the figures presented are very approximate estimates. The efficiency of the devices listed in Table 2 is also generally not available due to the limited information provided in the papers.

The prototype mechanism has been designed for under-floor use and was intended to allow easy adaptation to different springs and flywheel dimensions and was not designed to be compact. Given a particular set of parameters it would be possible to significantly reduce the overall size of the device. A key constraint on the miniaturisation is the volume of material required in the spring and flywheel energy storage elements in order for them to have sufficient energy storage capacity. In the current design, these have volumes of $6 \times 10^{-6} m^3$ and $42 \times 10^{-6} m^3$ respectively while the generator has a volume of $27 \times 10^{-6} m^3$. Other components of the system could be miniaturised through more careful design. The simulation model developed would allow a prediction of performance for different designs.

In addition to use in an under-floor situation, it would be possible to adapt the mechanism to use within a shoe. A typical shoe heel might have dimensions of $50 \times 50 \times 20mm$ and thus a volume of $50 \times 10^{-6} m^3$. The volume of a shoe heel is thus not significantly smaller than that required for the key components of the current device. However, considerable ingenuity would be required to reconfigure the mechanism to fit within the space available within a shoe and it is likely that it would be necessary to reduce the level of energy extracted.

CONCLUSIONS

A novel mechanism has been proposed which is capable of extracting significant levels of energy from normal human motion and converting this energy into electrical energy. The use of a spring and flywheel mechanism, along with a striker mechanism, enables an efficient velocity amplification which allows high-force, low-amplitude footfall motion to be matched to an electromagnetic generator which operates most efficiently at high speed. A mathematical model representing the behaviour of the mechanism in the four phases of its operation has been developed and using this, it has been possible to identify system parameters which optimise the output power and efficiency. Experimental results demonstrate an output energy of 450mJ per step with an efficiency of 11.5%. These figures compare favourably with the majority of published footfall devices. The current experimental system has been designed to allow easy parameter adjustment but it is believed that its size could be significantly reduced with further design effort.

REFERENCES

Donelan, J. M. , Li, Q., Naing, V. et al. 2008, “Biomechanical energy harvesting: Generating electricity during walking with minimal user effort”. Science Vol. 319. no. 5864, pp. 807 – 810, 8th Feb.

Gilbert, J.M. and Balouchi, F., 2008 “Comparison of Energy Harvesting Systems for Wireless Sensor Networks”, International Journal of Automation and Computing 05(4), pp. 334-347

Gilbert, J.M., Oldaker, R.S., Grindley, J.E. et al, 1996, “Control of a novel switched mode variable ratio drive”, *Int. Conf. UKACC 96,* Vol. 1, pp. 412 – 417, 2-5 September 1996, Exeter, UK, IEE publishing, Stevenage, UK.

Hassan, A.H.A., Gilbert, J.M. and Ishak, D., 2008, “Design and Testing of a Dual-Mode Mechanical Drive”, IEEE 5th International Symposium on Mechatronics and its Applications, Amman, Jordan.

Highway Energy Systems Ltd., http://www.hughesresearch.co.uk/, Accessed 21st August 2012.

Kymissis, J., Kendall, C., Paradiso, J. et al, 1998, “Parasitic Power Harvesting in Shoes”, *2nd IEEE Int. Conf. on Wearable Computing*, pp. 132-139.

Pelrine, R., 2002, http://handle.dtic.mil/100.2/ADA414020 accessed 2 June 2011

Pelrine, R., Kornbluh, R.D., Eckerle, J. et al, 2001, “Dielectric elastomers: generator mode fundamentals and applications”, *Proc. SPIE Vol. 4329 Smart Structures and Materials 2001: Electroactive Polymer Actuators and Devices, Ed. Yoseph Bar-Cohen,* , pp. 148-156, SPIE publishing Bellingham, WA USA

Portescap Motor/generator manufacturer data sheet http://www.portescap.com/brush-dc/product-89-28L28.html# accessed on 21st August 2012.

Priya, S. and Inman, D.J. (Ed), 2009, “Energy Harvesting Technologies”, Springer, New York, USA.

Shenck, N.S. and Paradiso, J.A., 2001, “Energy Scavenging with Shoe-Mounted Piezoelectrics”, *IEEE Micro*, Vol 21, No 3, pp30-42

Starner, T., 1996, “Human Powered Wearable Computing”, *IBM Systems Journal*, Vol. 35, No. 3/4, pp. 618-629.

Takefuji, Y. 2008a, “Known and unknown phenomena of nonlinear behaviors in the power harvesting mat and the transverse wave speaker”, Proc. of international symposium on nonlinear theory and its applications., Budapest, Hungary, September 7-10

Takefuji, Y. 2008b, “Et si les transports publics ne consommaient plus d’énergie?”, Le Rail, No 145, pp31-33.

Trew, M. and Everett, T., 2001, “Human Movement, 4th Ed”, Churchill Livingstone Elsevier.